Inductive Thermography – a non-destructive inspection technique

by B. Oswald-Tranta

* Chair of Automation and Measurement, University of Leoben, Peter-Tunnerstr.27, 8700 Leoben, Austria, *beate.oswald@unileoben.ac.at*

Abstract

Inductive thermography is an excellent inspection technique for detecting defects in metallic materials. The technique has been greatly improved over the last few decades, from laboratory experiments to industrial applications. Many researches have studied the theory and the physical equations behind inductive thermography. The purpose of this paper is to give an overview of the theory and also of the most important technical points which should be taken into consideration for the usage of this technique. Examples are given of how it is used in industrial inspections today.

1. Introduction

In the case of inductive thermography, a short inductive heating pulse is applied to the work-piece to be inspected and an infrared (IR) camera records its surface temperature. Due to the material's ohmic resistance, Joule heat is generated in the work-piece. Defects, such as cracks, affect both the eddy current distribution and the heat flow, making the defects visible in the IR images.

The technique can be used for inspecting electrically conductive materials. In most of the cases it is used for testing metals. However, since carbon fibres conduct electricity, CFRP structures can also be inspected by using inductive thermography. This paper focuses on the usage of inductive thermography to detect surface cracks in metals. After an overview of the physics behind the induction thermography, several technical aspects of the setup are discussed. The evaluation of the recorded IR sequence and the comparison with other techniques are then summarized. In the recent years, several approaches have been developed to fully automate the inspection, both in terms of specimen handling, and defect location and the characterisation. These results lead to industrial applications, some of which are described in the last section of the paper.

2. Eddy current flow around surface cracks

An alternating voltage is induced in a work-piece when it is placed in an alternating magnetic field. In an electrically conductive material, this further induces an electrical current known as eddy current. The induced eddy current decays exponentially below the surface, and it penetrates only into a thin skin, which is characterized by the penetration or skin depth:

$$\delta = \sqrt{\frac{1}{\pi \mu_0 \mu_r \sigma f}} \tag{1}$$

where μ_0 is the vacuum permeability of with a value of $4\pi 10^{-7}$ Vs/Am; μ_r is the relative magnetic permeability of the material; σ is its electrical conductivity and f is the excitation frequency. For austenitic steel, the skin depth is approximately 1.34 mm, at an excitation frequency of f = 100 kHz. For a typical ferro-magnetic steel, due to its magnetic property of μ_r = 600, the penetration depth is only 0.048 mm for the same excitation frequency.

The exponential decay function is strictly valid only for a semi-infinite long plane surface. For other geometries, such as the case around a surface crack, the eddy currents flow around the obstacle. To calculate the eddy current, the Joule heating and the temperature distribution for these situations finite element simulations can be used, such as ANSYS, which is able to couple the electromagnetic and the thermal processes in the modelling. It can be observed, that the current does not exactly follow the side of the work-piece, in the case of a corner the current flow is pushed away from the corner at a distance of about twice the penetration depth [1], see Figure 1a. Due to the ohmic resistance of the material along the eddy current flow Joule heating is generated, which furthermore results in an inhomogeneous heating around defects. The inhomogeneous Joule heating causes an inhomogeneous temperature distribution at the surface, which can be detected by an infrared camera, see Figure 1c and d. It is to emphasize that defects disturb as well the eddy current flow as the heat diffusion, therefore the temperature difference caused by a crack is much larger than in the case e.g. by laser heating, where only the lateral heat flow is disturbed by a defect, but not the heating process itself.

For ferro-magnetic materials, the penetration depth is very small compared to the depth of a surface crack being inspected, so the inductive heating can be modelled as a surface heating, that also occurs along the crack sides in the material, see Figure 1b. The assumption of a surface heating allows even an analytical modelling of the inductive

thermography [2]. Due to the heat accumulation in the corners of a surface cracks, in ferro magnetic materials a crack can be detected due to higher temperature at the surface (Figure 1d).

On the other hand, in non-magnetic materials, where the eddy current penetration depth is comparable to or greater than the typical surface crack depth, it has a significant effect that the eddy current flow is at the corner of the crack far from the surface. As the current flow is pushed away from the crack, there is locally less Joule heating around the crack, which can be detected by lower temperature values, see Figure 1a and c.

The deeper a crack is, the greater the obstacle it represents for the eddy currents and also for the heat diffusion. Therefore, the temperature perturbation in the vicinity of a crack is significantly related to its depth. This is one of the main advantages of the inductive thermography: the measured signal strength can be used to estimate the depth of the crack below the surface [1].

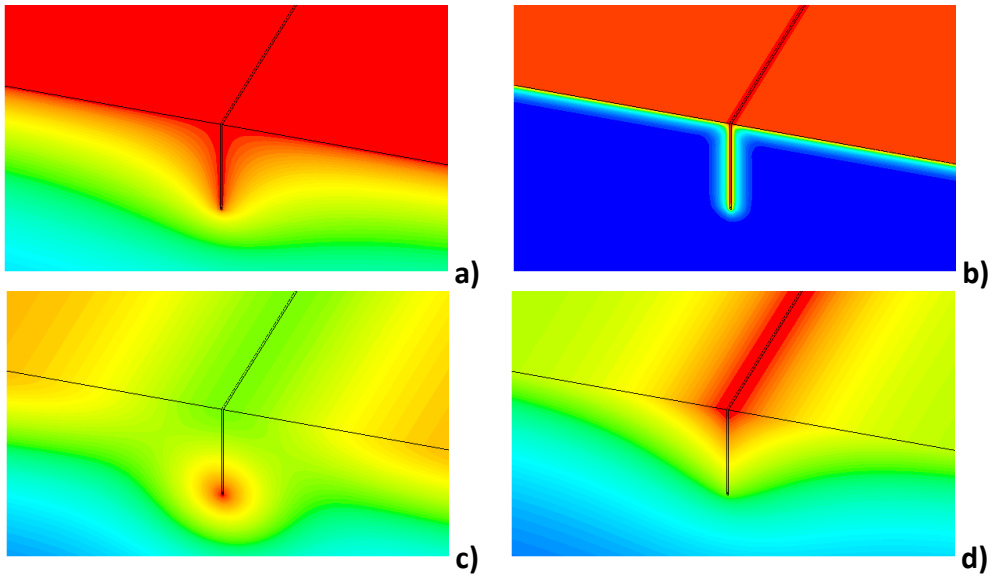

Figure 1: Simulation results for a 1mm deep crack: eddy current distribution in non-magnetic AISI steel (a) and in ferro-magnetic steel (b) by 100 kHz excitation frequency; temperature distribution after 0.1 s heating pulse in non-magnetic AISI steel (c) and in ferro-magnetic steel (d)

The previous statements treated a crack as a long crack, without considering the effects around the crack tip at the surface. Figure 2a shows the temperature around a 3 mm long surface crack in a non-magnetic austenitic steel specimen. In the central part of the crack, the eddy current flows below the surface, resulting in a lower temperature value than at the defect-free surface, in similar way as it is for a long crack. However, around the crack tip there is a higher current density, resulting in a high temperature hot spot.

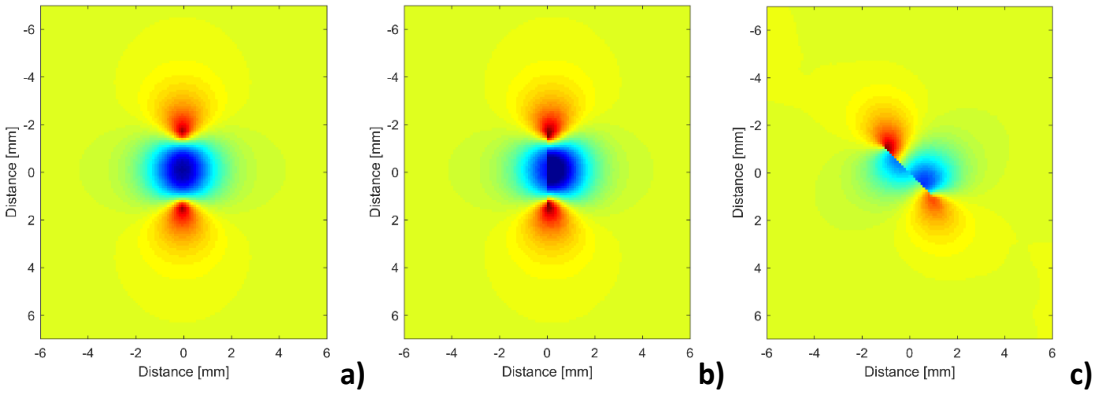

Figure 2: Simulated temperature results for a 3 mm long and 1 mm deep crack after 100 ms inductive heating pulse: crack is perpendicular to the surface and to the eddy current direction(a); crack has an inclination angle of 30° and perpendicular to the eddy current direction (b) and having 45° to the eddy current direction (c).

The inclination angle of the crack also affects the eddy current as well as the heat diffusion. The cracks discussed previously penetrated the material perpendicularly. If the crack has an inclination, then the observed temperature pattern on the both sides the crack will not be symmetrical [3], see Figure 2b.

When the induced eddy current hits the crack at 90°, the disturbance caused by the crack is the greatest. This case has been demonstrated in the previous figures. If the angle between the crack line and the eddy currents is less than 90°, then the pattern is rotated [3], see Figure 2c. However, if the eddy currents flow parallel to the crack line, then the crack is no longer an obstacle to the current and no temperature perturbation due to the crack can be observed. This type of problem is well known from magnetic particle testing, where if the magnetization is parallel to the crack line, then the crack cannot be detected.

3. Experimental setup

The two main hardware components required for inductive thermography inspection are an infrared camera and an induction generator with inductor. There are two types of generators commonly used: one with a water-cooled copper coil, and one with an air-cooled ferrite core inductor, see Figure 3. The first type of generator operates as a resonant circuit. Internal capacitors and the external copper coil together with the sample form a resonant circuit, and the excitation frequency of the generator is close to this resonance frequency. This type of generator can provide large induction power, even up to 20 kW is possible. On the other hand, the copper coil carries a large electrical current and therefore needs to be water cooled. The coil is made of a copper tube with water cooling inside. This generator is able to produce power in a large space, where e.g. a work piece can be placed inside the coil. Figure 3a shows a so-called Helmholtz coil, which has the advantage, that the magnetic field between the two windings is almost homogeneous [5]. This type of generator has the disadvantage, that the excitation frequency cannot be easily changed: additional capacitors can be added or the geometry of the copper coil can be modified, but then the output working frequency is fixed. The usual working frequency range of this type of generators is between 40 kHz and 200 kHz.

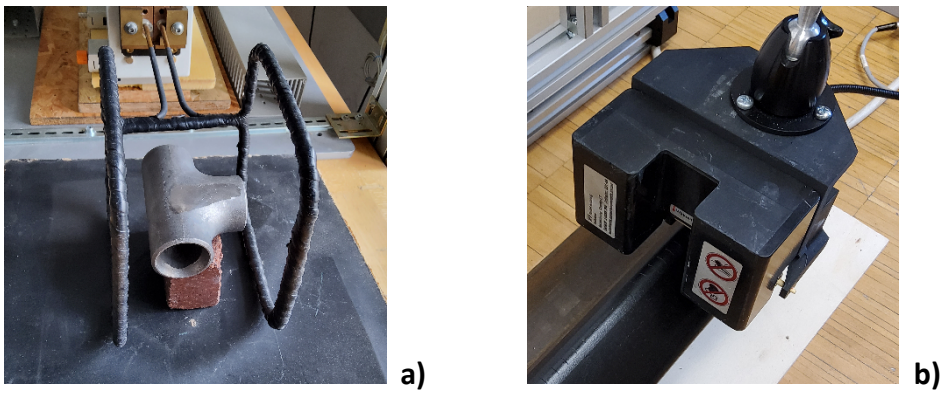

Figure 3:Two types of inductors: a) water-cooled Helmholtz coil; b) air-cooled ferrite-core inductor

The second type of generator uses frequency and pulse width modulation, with copper wires wrapped around a ferrite core, which normally does not need to be cooled [4]. The output frequency can be set by software via control parameters, e.g. in a range between 25 kHz and 60 kHz. The spatial area of the excitation is small, determined by the size of the ferrite core, see Figure 3b. However, this type of generator has the advantage of being easy to use, as no water cooling is required.

As mentioned above, the detectability of the crack depends on the angle between the orientation of the induced magnetic field and the crack. In a general setup, in order to detect any crack orientation, two measurements are required, with two different magnetic field orientations at 90° to each other. There have been some suggestions as to how the measurement can be made without rotating the inductor. In the case of water-cooled Helmholtz coil setup, it is possible to use two such kind of coils with slightly different excitation frequencies. In this way the magnetic field rotates describing Lissajous curves, and any crack orientations can be detected [5]. For the generators with ferrite core inductor, it is possible to design the ferrite cores in such a way, that there are separate ferrite cores with copper windings included in one inductor, and they are responsible to generate the magnetic field in different directions. The different windings on the different ferrite cores are then electrically switched on one after the other. In this way no movement of the inductor is required, and the different magnetic field orientations are automatically measured [6], [7].

Both types of generator can be used in a static or in a scanning mode. In static mode none of the components move and the IR camera records the surface temperature during the heating pulse. In many cases it has been found advantageous to record the surface temperature not only during the heating pulse but also afterwards, during the cool down phase. The whole recorded IR sequence, i.e. the temporal change of the temperature for each pixel, is then analysed. Usually a short inductive pulse, between 50 ms and 1 s, is applied. The shorter the pulse, the sharper the contrast as there is less time for the temperature difference to equalise due to heat diffusion. On the other hand, a shorter heating pulse means less induced energy, which in turn means less signal and more noise. The optimum choice of heating pulse length is an important factor, determined by the experimental setup and by the defects to be detected.

In the case of scanning mode there is a relative movement between the inspected sample and the inductor. The IR camera remains fixed to the excitation. This type of method is used, when inspecting long pieces such as semi-finished products, as steel billet or rails. As the camera is recording the temperature from a different area of the specimen due to

the movement, either the temperature images themselves are analysed or the recorded sequence has to be reordered to obtain a quasi-static IR sequence.

4. Evaluation of the infrared images

In the case of static measurement, the temporal change in temperature is recorded during the heating pulse and also during the cooling time. If only one single temperature image at the end of the heating pulse is evaluated, it will be affected by negative effects, such as inhomogeneous heating and inhomogeneous emissivity of the surface. The most practicable to reduce these effects is to use the PPT technique [8] and calculate a phase value for each pixel by applying the Fourier transform:

$$F_\tau = \int_0^\tau T(t) e^{\frac{-i2\pi t}{\tau}} dt \tag{2}$$

$$\varphi = \arctan \frac{\mathrm{Im}(F_\tau)}{\mathrm{Re}(F_\tau)} \tag{3}$$

where $\tau = t_{pulse} + t_{cooldown}$. The duration of $t_{cooldown}$ is usually chosen to be equal to t_{pulse}. Note that since the recorded IR sequence is not continuous, the Fourier transform is calculated by using the Discrete Fourier Transform (DFT). Due to the normalization of the phase calculation, the above mentioned inhomogeneity effects are strongly reduced [9].

Originally, the PPT technique has been developed to detect subsurface defects by applying optical heating with a flash lamp. In the case of subsurface defects, the thermal waves are reflected from different depths of the defects. Therefore, several frequencies of the Fourier transform spectrum are analysed as their behaviour gives information about how deep the defect is below the surface. In the case of surface crack detection using inductive thermography, the physical meaning of the phase values is different. It does not represent the phase shift of the thermal waves due to reflection from the depth, but rather it shows, how fast or slow the heating and cooling occurs at each pixel location [9].

As mentioned in the previous section, shorter heating pulses produce sharper images because there is less time for the heat to diffuse. On the other hand, the short heating pulse delivers less energy, which can lead to noisy images, especially for non-magnetic materials, where the inductive heating is less efficient. Similar to the lock-in technique developed to detect subsurface defects by applying sinusoidal thermal heating over several periods [10]-[14], this technique can also be adapted to inductive thermography [15],[16]. Several heating pulses are applied in succession and the phase value is calculated for the frequency of 1/τ:

$$F_{n,N_{pulse}} = \frac{2}{n \cdot N_{pulse}} \cdot \sum_{j=1}^{N_{pulse}} \sum_{k=0}^{n} T_k \, e^{-2\pi k i / n} \tag{4}$$

where n is the number of images recorded during one period and N_{pulse} is the number of pulses recorded. It can be shown, that this calculation reduces the noise by $\sqrt{n \cdot N_{pulse}}$, i.e. the higher the IR camera's recording frame rate and the more pulses are recorded, the better the noise reduction [14], [16]. Figure 4 illustrates this effect: 10 consecutive heating pulses, each of them with 100 ms duration, were applied to the sample. After each heating pulse an additional 100 ms is recorded during the cooling time. Figure 4a shows the phase image evaluated for the first heating pulse only. In Figure 4b all the ten heating pulses are evaluated, for the same frequency of 1/(2 * 100 ms) = 5 Hz. It can be observed, that the noise is strongly reduced by evaluating ten pulses, and so the cracks become clearer detectable.

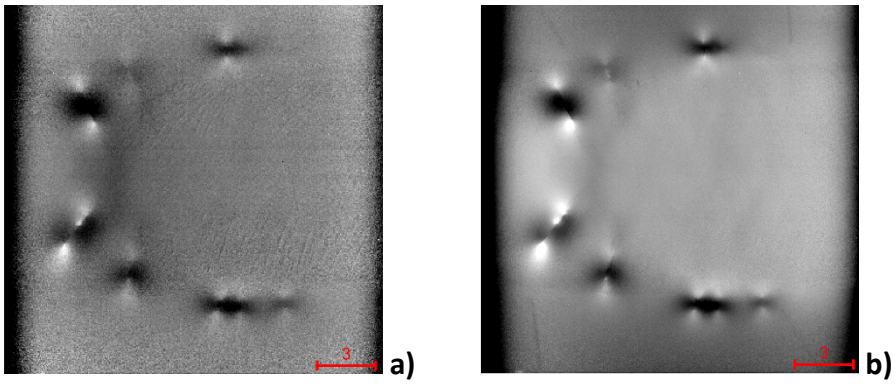

Figure 4: Phase image of a weld with small surface cracks after one heating pulse (a) and after 10 pulses (b).

In the case of scanning measurements, the IR camera records the temperature of different positions on the sample. Therefore, the Fourier transform described above cannot be applied directly. By reordering the IR sequence according to the spatial shift between two recorded images, a quasi-static IR sequence can be generated. The Fourier transform can then be applied to this sequence with the same advantages as for the static measurement [17].

5. Combination with other techniques

IR images show the temperature distribution of the surface, but many details of the object are not visible, if they have the same temperature. This sometimes makes it difficult to interpret the IR images. It is therefore a great advantage to use a visible camera in addition to the IR camera, and fuse the images from both [18],[19]. In many cases it is helpful, if the object edges localized in the visual images are also shown in the IR images [20]. Also in the case of inductive thermography it helps to interpret the IR results, by combining the images from both types of cameras. It is very helpful in locating the defects on the real work-piece, after they have been detected in the IR image [21].

The 3D geometry of a work-piece can be measured, e.g. by using the light sectioning technique. The combination of the 3D data and the inductive thermography results, also supports the localizing the defects on the sample [22], see Figure 5a. An additional advantage can be that artefacts, caused by strong edges of the sample can be identified and filtered out due to the 3D data.

The real size, as depth and shape of the defects below the surface can be measured by computed tomography (CT). Combining such CT results with the inductive thermography results can be used excellently to see what kind of phase patterns the different cracks produce [23], see e.g. Figure 5b.

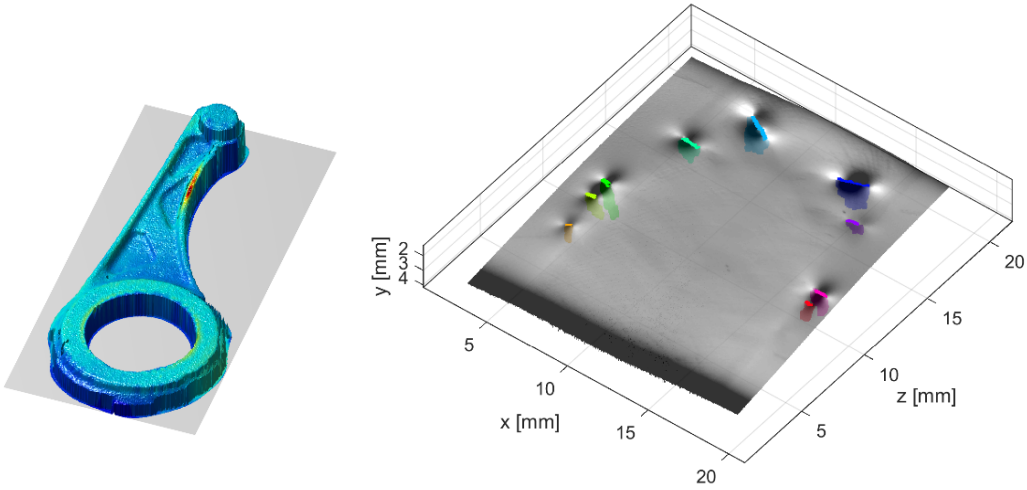

Figure 5: a: 3D surface of a level measured by light-sectioning and combined with thermographic results, revealing a surface crack by higher temperature; b: CT results of a sample with the detected cracks, combined with the phase image of the sample.

6. Automatic defect detection

In order to achieve a fully automated inspection, the defects have to be located automatically in the images. If the images have a strong signal-to-noise ratio, then it is possible to locate the defects e.g. with the edge detection technique. Figure 6 shows such an example, where railway rail was inspected using inductive thermography and the defects are very well visible and could be automatically located [24].

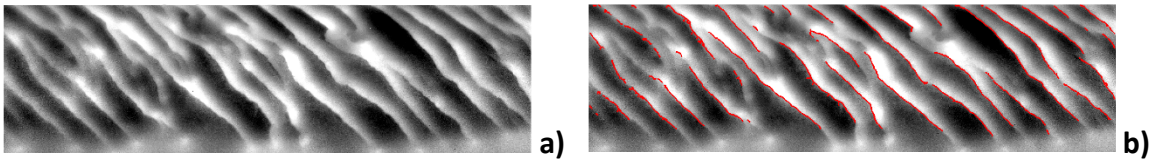

Figure 6: Phase image of a rail head with rolling contact fatigue cracks (a), the recognised crack lines are marked by red lines (b) [24]

Castings or forgings have a complex geometry with several edges. In such a case not only the defects, but also the edges become warmer due to the inductive heating. In Ref.[25] in a first step the hot patches are segmented and then several features such as temperature increase, compactness, concavity have been used to train a neural network (NN). This NN is able then to classify, whether the patch is caused by a crack or by the geometrical edge of the part, see Figure 7.

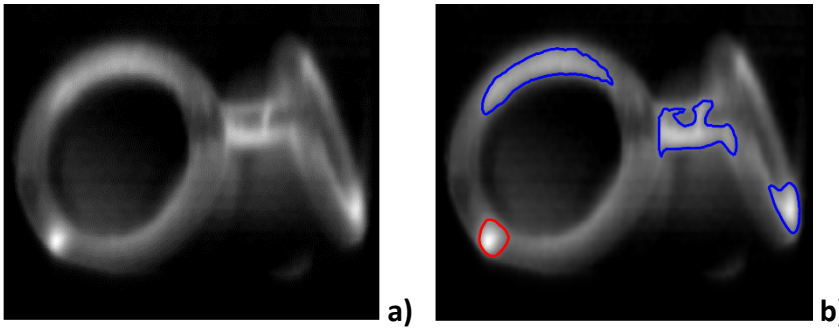

Figure 7: a: Temperature image of a casting after short inductive heating pulse; b: four warm patches have been identified, one of them was classified as a crack (red line) and three of them as caused by geometry [25]

In the recent years, several deep learning techniques have been developed. They have also been applied to defect detection in thermographic inspection. Here are a few examples that have been proposed for use in inductive thermography:

- In Ref.[26] defects at the backside of a sample are detected by using inductive thermography. In order to improve the images an autoencoder has been trained.
- For detecting surface cracks in welding the temperature images after a short inductive heating pulse was used in Ref.[27]. As the crack lines have higher temperature than the surrounding surface, a transfer learning was proposed based on public data bases for retinal vessel images.
- To detect cracks in forged parts by a U-net, parts with typical surface cracks were used in Ref.[28]. Based on the phase images, half of the 44 parts were used to train the network, and the other parts to evaluate the network performance by intersection over union (IoU) metric.
- In Ref.[29] phase images of inductive thermography results were used to locate the defective areas around the cracks. A convolutional neural network (CNN) was trained on simulation data with additional noise, and this network was used for semantic segmentation of the experimental results of welded samples. Figure 8 shows such an example, where first the image is segmented, as the network recognizes the patterns around the short cracks. In the next step, these regions are enlarged and then inside the bounding polygons the crack length, the phase minima and maxima are determined. These values will then be used for the characterization of the cracks.

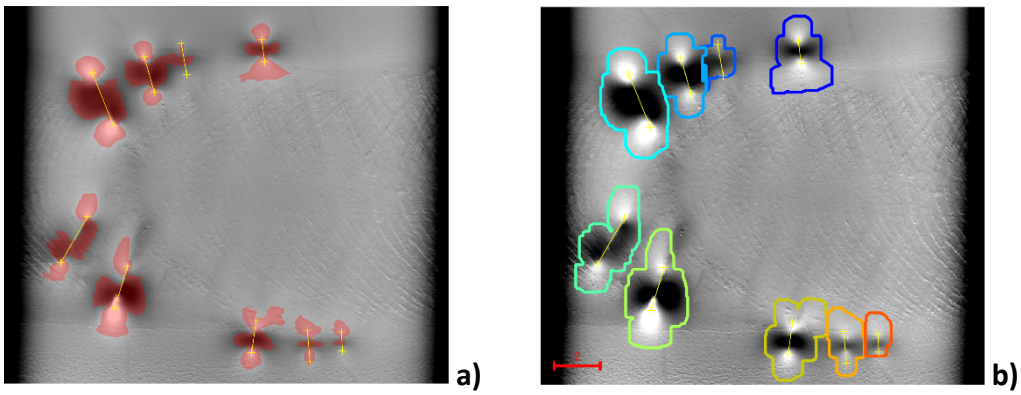

Figure 8: a: Semantic segmentation of a sample with nine surface crack regions; b: Marking with lines around the crack regions.

7. Industrial applications

Traditionally, for inline non-destructive testing for surface crack detection, one of two inspection techniques is used: magnetic particle inspection for ferromagnetic materials or liquid penetrant inspection for non-magnetic materials. Both of these techniques are usually performed manually by humans, both do not provide information on depth of the crack in the sample, and both require several chemicals, that are not environmentally friendly. Inductive thermography has great potential to replace these two methods in industrial applications.

In the early 1980s, a commercial inspection system, called Therm-O-Matic, was offered for detecting surface cracks in steel bars and billets [30]. The long objects were moved through an induction coil at a speed of approximately 1 m/s and four line scan IR cameras recorded the temperature at the four sides of the billet behind the induction coil. These

temperature profiles were analyzed to locate surface cracks. To reduce the inhomogeneous emissivity of the surface, the specimen was moistened with water prior to inductive heating. This system has been developed further first by Corus Research [31] and then by Foerster [32], using FPA IR cameras instead of line scan cameras. Based on the recording of the 2D IR images, the temporal change of the temperature can be analysed. This improves the defect detectability.

Induction thermography is an excellent method of inspecting welds [33][34]. This can be done in a two-sided mode, where the IR camera and the induction coil are placed on different sides of the weld, and the heat flow through the weld is analysed to locate and characterize different defect types. If the weld is only accessible from one side, then inductive thermography can be used to detect surface cracks in the welds [33]-[37].

Forgings and castings, produced specifically for the automotive industry must be 100% inspected for possible defects. Also other parts, as generator components, compressor blades, or other aircraft engine components have high safety requirements. As these parts often have complex geometries, manual inspection by humans using magnetic particle inspection or fluorescent penetrant inspection is used. However, inductive thermography has been shown to have great potential here, due to its ability to be highly automated and to provide information on the depth of surface cracks [22],[38]-[45].

Railway inspection is another very important area. Nowadays rails are typically inspected using eddy current testing for surface cracks, and ultrasonic testing for volumetric defects. Inductive thermography also has a great potential in this area, as several papers published in the recent years have shown [24], [45]-[51].

For industrial applications, it is important to have a standard for the inspection. In Germany there is already a standard available for inductive thermography since 2018 [44],[45], [52]. This standard will soon be also available in Europe through the work of the European Committee for Standardization (CEN).

8. Summary

Inductive thermography has been greatly improved over the last few decades, and it is increasingly being used also in the industry for NDT inspection. The method is non-contact, fast, and the inspection process and the evaluation can be fully automated. The development of new different inductors, from water-cooled copper coils with different geometries to air-cooled inductors with ferrite cores, allows the technique to be scaled and adapted to the task. IR cameras have also improved greatly in the recent years, with better temperature resolution and higher record frequency, with smaller sizes and with lower prices. These trends are opening up more and more opportunities for industrial applications.

REFERENCES

[1] Oswald-Tranta, B. ”Induction thermography for surface crack detection and depth determination”, *Applied Sciences* (Switzerland), 8 (2), 257, 2018; *doi:10.3390/app8020257*

[2] Oswald-Tranta B., “Thermo-inductive crack detection,” *J. Nondestructive Testing and Evaluation*, vol. 22, no. 2, pp. 137–153, 2007.

[3] Oswald-Tranta, B. Detection and characterisation of short fatigue cracks by inductive thermography. *QIRT J. Vol.19(4) pp 239-260,* **2021**. https://doi.org/10.1080/17686733.2021.1953226

[4] IFF GmbH, Available online: https://www.iff-gmbh.de/en/induction-technology/generatoren/, (accessed on Mai.2024)

[5] Oswald-Tranta B. and Sorger M., “Localizing surface cracks with inductive thermographical inspection: from measurement to image processing,” *QIRT Journal*, vol. 8, no. 2, pp. 149–164, 2011.

[6] Tang, B., Hou, D., Hong, T. & Ye, S. Influence of the external magnetic field on crack detection in pulsed eddy current thermography. *Insight* **60**, 240–246. https://doi.org/10.1784/insi.2018.60.5.240 (2018).

[7] Urtasun, B., Andonegui, I. & Gorostegui-Colinas, E. Phase-shifted imaging on multi-directional induction thermography. *Sci Rep* **13**, 17540 (2023). https://doi.org/10.1038/s41598-023-44363-5

[8] Maldague, X., Marinetti, S.: Pulse phase infrared thermography. J.Appl. Phys. 79(5), 2694–2698 (1996)

[9] Oswald-Tranta B., “Time-resolved evaluation of inductive pulse heating measurements,” *QIRT Journal*, vol. 6, no. 1, pp. 3–19, 2009. https://doi.org/10.3166/qirt.6.3-19

[10] Wu D, Busse G. Lock-in thermography for nondestructive evaluation of materials. Rev Gen De Therm. 1998;37(8):693–703.

[11] Maierhofer C, Myrach P, Krankenhagen R, et al. Detection and characterization of defects in isotropic and anisotropic structures using lockin thermography. J Imaging. 2015;1 (1):220–248.

[12] Meola C, Carlomagno GM, Squillace A, et al. Non-destructive evaluation of aerospace materials with lock-in thermography. Eng Fail Anal. 2006;13(3):380–388.

[13] Sakagami T, Kubo S. Applications of pulse heating thermography and lock-in thermography to quantitative nondestructive evaluations. Infrared Phys Technol. 2002;43(3–5):211–218.

[14] Breitenstein O, Langenkamp M. Lock-in thermography. In: K Itoh, T Lee, T Sakurai, WMC Sansen, D Schmitt-Landsiedel, editors. Springer series in advanced microelectronics. Berlin Heidelberg: Springer Verlag; 2003.

[15] Riegert G, Zweschper T, Busse G. Lockin thermography with eddy current excitation. QIRT J. 2004;1(1):21–31.

[16] Oswald-Tranta, B. “Lock-in inductive thermography for surface crack detection in different metals”, QIRT Journal, 16 (3-4), pp. 276-300. (2019) https://doi.org/10.1080/17686733.2019.1592391

[17] Oswald-Tranta B. and Sorger M., “Scanning pulse phase thermography with line heating,” QIRT Journal, vol. 9, no. 2, 2012.
[18] Ma, W., Wang, K., Li, J., Yang, S. X., Li, J., Song, L. and Li, Q., “Infrared and Visible Image Fusion Technology and Application: A Review,” Sensors 23(2), 599 (2023).
[19] Sun, C., Zhang, C. and Xiong, N., “Infrared and Visible Image Fusion Techniques Based on Deep Learning: A Review,” Electronics 9(12), 2162 (2020).
[20] Teledyne FLIR MSX, Available online: https://www.flir.eu/discover/professional-tools/what-is-msx/, (accessed on Mai.2024)
[21] Tuschl C., Agathocleous T., Oswald-Tranta B., Eck S., "Scanning inductive thermography using a μ-bolometer and a visual camera," Proc. SPIE 12536, Thermosense: Thermal Infrared Applications XLV, 125360D (12 June 2023); doi: 10.1117/12.2662819
[22] Oswald-Tranta B. and O’Leary P., “Fusion of geometric and thermographic data for automated defect detection,” J. Electron. Imaging, vol. 21, 2012.
[23] Oswald-Tranta B., Hackl A., Gorostegui-Colinas E., Muniategui Merino A., Westphal Ph., "Inspection of short surface cracks by inductive thermography and by computer tomography," Proc. SPIE 13047, Thermosense: Thermal Infrared Applications XLVI, (2024)
[24] Tuschl, C., Oswald-Tranta, B., Eck, S., „Inductive thermography as Non-Destructive Testing for railway rails“, Appl. Sci. **2021**, 11, 1003. https://doi.org/10.3390/app11031003
[25] B. Oswald-Tranta, M. Sorger, and P. O’Leary, “Thermographic crack detection and failure classification,” J. Electron. Imaging, vol. 19(3), no. July-Sep, 2010.
[26] Xie, J., Xu C., Chen G. Huang W. “Improving visibility of rear surface cracks during inductive thermography of metal plates using Autoencoder”. Infrared Physics & Technology, 2018. 91: p. 233-242.
[27] R. Moreno, E. Gorostegui, P. López de Uralde, A. Muniategui, “Towards automatic crack detection by Deep learning and active thermography”, chapter in book Advanced in Computational Intelligence, 151-162, 2019, DOI: 10.1007/978-3-030-20518-8_13
[28] D. Müller, U. Netzelmann, B. Valeske,” Defect shape detection and defect reconstruction in active thermography by means of two-dimensional convolutional neural network as well as spatiotemporal convolutional LSTM network”, QIRT Journal, 19:2, 126-144, DOI: 10.1080/17686733.2020.1810883 (2022)
[29] Oswald-Tranta, B.; Lopez de Uralde Olavera, P.; Gorostegui-Colinas, E.;Westphal, P. Convolutional neural network for automated surface crack detection in inductive thermography. In Proceedings of the SPIE, Thermosense: Thermal Infrared Applications XLV, Orlando, FL, USA, 30 April–4 May 2023; Volume 12536.
[30] Kremer, K., et al., „Das Therm-O-Matic-Verfahren - ein neuartiges Verfahren für die Online-prüfung von Stahlerzeugnissen auf Oberflächenfehler“, Stahl Eisen 105, 39–44 (1985). (in German)
[31] Wullink J., Darses Ph., “On-line thermography applied to crack detection in steel billets”, in Proc.QIRT conf. 2000.
[32] Koch S., Schroeder J., “In-Line Inspection of Hot-Rolled Steel Billets by Heat Flux Thermography”, in Proc. of 11th QIRT conf., Neapel, Italy, 2012
[33] Srajbr, Ch., “Induction excited thermography in industrial applications”, in Proc. of 19th WCNDT conf., Munich, Germany, 2016
[34] Prints, E., Kryukov, I., Mund, M., Srajbr, C., Dilger, K., & Böhm, S. “Potential of Active Thermography as a Non-Destructive Testing Method for Quality Assurance of Welded Joints”, 2nd European NDT & CM Days, Oct 4-7, 2021, Prague, Czech Republic. https://www.ndt.net/?id=26437
[35] Eider Gorostegui-Colinas, Rafael Hidalgo-Gato, Pablo López de Uralde, Beñat Urtasun Marco, Ander Muniategui Merino, "Induction thermography based inspection of EBW and TIG welded Inconel 718 components: steps towards industrialization," Proc. SPIE 11409, Thermosense: Thermal Infrared Applications XLII, 114090D (18 May 2020); doi: 10.1117/12.2558265
[36] Gorostegui-Colinas, E., Muniategui, A., de Uralde, P. L., Gorosmendi, I., Heriz, B., and Sabalza, X., “A novel automatic defect detection method for electron beam welded inconel 718 components using inductive thermography," in Proc. of 14th QIRT conf., Berlin, Germany, 2018
[37] DIN 54186:2022–09 Non-destructive Testing – Testing of laser-beam welded joints using active thermography; Available online: https://www.din.de (accessed on Mai.2024)
[38] Goldammer M., Mooshofer H., Rothenfusser M., Bass J., Vrana J., “Automated Induction Thermography of Generator Components”. AIP Conference Proceedings, vol. 1211, pp. 451 – 457, 2010, DOI: 0.1063/1.3362428.
[39] Vrana J., Goldammer M., “Active Thermography with Electromagnetic Excitation: Defect-Specific Warming and Underlying Current Flow”, in Proc. of 14th QIRT conf., Berlin, Germany, 2018
[40] G. Zenzinger, J. Bamberg, W. Satzger & V. Carl (2007) “Thermographic crack detection by eddy current excitation, Nondestructive Testing and Evaluation, 22:2-3, 101-111, DOI: 10.1080/10589750701447920
[41] M. Genest and G. Li, "Inspection of Aircraft Engine Components Using Induction Thermography," 2018 IEEE Canadian Conference on Electrical & Computer Engineering (CCECE), Quebec, QC, Canada, 2018, pp. 1-4, doi: 10.1109/CCECE.2018.8447832.
[42] P. Bouteille, G. Legros, “Induction thermography as an alternative to conventional NDT methods for forged Parts”, in Proc. of 12th QIRT Conf., Bordeaux, 2014.
[43] Netzelmann U, Walle G. Induction thermography as a tool for reliable detection of surface defects in forged components. Proc. 17th World Conference on Nondestructive Testing; 2008 Oct 25–28;

Shanghai, China.
[44] U.Netzelmann, G.Walle, S.Lugin, A.Ehlen, S.Bessert, B.Valeske, “Induction thermography: principle, applications and first steps towards standardisation”, QIRT Journal 13(2), 170-181, (2016)
[45] U. Netzelmann, “Induction Thermography of Surface Defects” in Handbook of Advanced Nondestructive Evaluation, Springer International Publishing, Cham, 2019, pp. 1497-1522, https://doi.org/10.1007/978-3-319-26553-7
[46] J.Wilson, G.Tian, I.Mukriz, D.Almond, “PEC Thermography for Imaging Multiple Cracks from Rolling Contact Fatigue”, NDT & E International, 44(6), 505-512, (2011)
[47] Peng, J., Tian G.Y., Wang L., Zhang Y., Li K., Gao, X, “Investigation into eddy current pulsed thermography for rolling contact fatigue detection and characterization”. NDT & E Int. 74, 72–80 (2015).
[48] Li H., Gao B., Lu X., Zhang X., Shi Y., Ru G., Woo W., “Dynamic Rail Near-surface Inspection of Multi-physical Coupled Electromagnetic and Thermography Sensing System”, IEEE Transactions on Instrumentation and Measurement, vol. 72, pp. 1-13, 2023
[49] Tuschl, C., Oswald-Tranta, B., Eck, S., & Dornig, P. „Scanning pulse phase thermography for surface defect detection in manganese steel turnout frogs”. in Proc. of the European Conference on Non-Destructive Testing (ECNDT) from 3 to -7 of July 2023 in Lisbon, Portugal. *Research and Review Journal of Nondestructive Testing* Vol. 1(1). https://doi.org/10.58286/28220
[50] Vaibhav, T., Balasubramaniam, K., Kidangan, R. and Bose, A., “Eddy current thermography for rail inspection,” 13th QIRT Conference, Gdansk,Poland (2016).
[51] D’Accardi, E., Dell’Avvocato, G., Masciopinto, G., Marinelli, G., Fumarola, G., Palumbo, D., & Galietti, U. (2024). Evaluation of typical rail defects by induction thermography: experimental results and procedure for data analysis during high-speed laboratory testing. *QIRT Journal*, 1–22. https://doi.org/10.1080/17686733.2024.2340060
[52] DIN 54183:2018–02, Non-destructive testing-Thermographic testing- Eddy-current excited thermography; Available online: https://www.din.de (accessed on Jan.2018)